

Seismic Response Analysis of Multiple-Frame Bridges with Unseating Restrainers
Considering Ground Motion Spatial Variation and SSI

by

Bipin Shrestha, Hong Hao and Kaiming Bi

Reprinted from

Advances in Structural Engineering

Volume 18 No. 6 2015

Seismic Response Analysis of Multiple-Frame Bridges with Unseating Restrainers Considering Ground Motion Spatial Variation and SSI

Bipin Shrestha*, Hong Hao and Kaiming Bi

Centre of Infrastructure Monitoring and Protection, Department of Civil Engineering, Curtin University, Bentley, Australia

(Received: 12 Jul 2014; Received revised form: 10 Sep 2014; Accepted: 11 Sep 2014)

Abstract: Unseating damages of bridge decks have been observed in many previous major earthquakes due to large relative displacement exceeding the available seat length. Steel cable restrainers are often used to limit such relative displacements. Present restrainer design methods are based on the relative displacements caused by the different dynamic characteristics of adjacent bridge structures. However, the relative displacements in bridge structures are not only caused by different dynamic characteristics of adjacent bridge segments. Recent studies indicated that differential ground motions at supports of bridge piers and Soil Structure Interaction (SSI) could have a significant influence on the relative displacement of adjacent bridge components. Thus the present design methods could significantly underestimate the relative displacement responses of the adjacent bridge components and the stiffness of the restrainers required to limit these displacements. None of the previous investigations considered the effects of spatially varying ground motions in evaluating the adequacy of the restrainers design methods. Moreover, the code recommendation of adjusting the fundamental frequencies of adjacent bridge structures close to each other to mitigate relative displacement induced damages is developed based on the uniform ground motion assumption. Investigations on its effectiveness to mitigate the relative displacement induced damages on the bridge structures subjected to spatially varying ground motion and SSI are made. This paper discusses the effects of spatially varying ground motions and SSI on the responses of the multiple-frame bridges with unseating restrainers through inelastic bridge response analysis.

Key words: spatially varying ground motion, soil-structure interaction, multiple-frame bridges, pounding, restrainers.

1. INTRODUCTION

During an earthquake, adjacent bridge segments can vibrate out-of-phase because of their different dynamic characteristics and variations in the ground motion inputs at multiple bridge supports. The out-of-phase motion results in two main problems. Firstly, when the relative displacement between the bridge segments exceeds the available seat width, unseating of the bridge span occurs. Many cases of bridge collapse that occurred in recent earthquakes were attributed to this

phenomenon (Saiidi *et al.* 1993; Moehle 1995; Comartin *et al.* 1995; Kawashima *et al.* 2011). On the other hand, when the bridge spans vibrate towards each other pounding might occur if the relative displacement is larger than the expansion gap size. Pounding could cause significant impact forces that can result in local damages and crushing of concrete. Additionally, large impact forces can increase opening at hinges between simply supported spans or at in-span hinges, which in turn could increase the possibility of unseating of the bridge spans.

*Corresponding author. Email address: bipinsh01@gmail.com; Tel: +61-411-727896.

Unseating of bridge decks during the 1971 San Fernando earthquake in the USA was a major reason behind the collapse of several bridges. This earthquake triggered the development of seismic restrainers to prevent the excessive relative movement of girders at superstructure hinges and at girder supports. Seismic restrainers since then have been installed as a retrofit measure in bridges with narrow supports to restrict the movement. It has also been used in new bridges with wide supports as a backup system. Steel cables and high strength steel rods attached to steel connections are the most widely used restrainer types. During the earthquakes such as the 1989 Loma Prieta, 1994 Northridge and 1995 Kobe earthquake restrainers were found effective in protecting the bridges against the unseating failures. However, a few bridges that had been retrofitted with cable restrainers still collapsed due to the unseating at hinges (Moehle 1995), indicating better understanding the performances of restrainers during strong shaking and improvement in the design are needed. Many researchers have since carried out researches to understand the influencing factors on the behaviour of restrainers and its influence on the overall performance of the bridge structures and to provide appropriate design procedure for restrainers. Saiidi *et al.* (1996) investigated four bridges retrofitted with cable restrainers during the 1989 Loma Prieta earthquake and concluded that the performances of restrainers were affected by many factors such as the amplitude and frequency contents of the ground motion, foundation flexibility as well as flexibility of the substructure and recommended that nonlinear time history analysis is necessary to design appropriate restrainers. Trochalakis *et al.* (1997) conducted 216 non-linear time history analyses for various frames, abutments, and restrainer properties and showed that the maximum relative displacement was sensitive to the stiffness of adjacent frames, the frames' effective periods, and the restrainer properties. DesRoches and Fenves (2000, 2001) suggested a new design procedure for steel restrainers and compared it with the results from nonlinear time history analyses. DesRoches and Muthukumar (2002) carried out a comprehensive study on the effects of pounding and restrainers on seismic response of multiple-frame bridges. It should be noted that all these studies neglected the effects of ground motion spatial variations, which, as will be demonstrated later in this paper, might be the detrimental factor that generates relative displacement between bridge spans.

As mentioned, most of the previous studies neglected the relative displacement arising from the non-uniform ground motions thus could underestimate the relative response of adjacent structures. For example, the design

method of the restrainers developed by DesRoches and Fenves (2000) takes into account only the out-of-phase vibration caused by different fundamental vibration frequencies of adjacent bridge components. As a result, it could underestimate the required stiffness and strength of the restrainers when subjected to spatially varying motion. This is realized by the current Caltrans code (Caltrans 2010), which states that "a satisfactory method for designing the size and number of restrainers required at expansion joints is not currently available". Researches on the response of bridge structure with cable restrainers to spatially varying ground motion including the SSI effect are inexistent. Though Won *et al.* (2008) investigated the effects of restrainers and pounding on the bridge responses subjected to non-uniform ground motion, due to the complexity of modelling coherency losses the study considered only the wave passage effect of spatial ground motion variations. Shrestha *et al.* (2014) presented the comparison of the response of different restrainers to spatially varying ground motions, in which ground motion spatial variation was modelled in detail. However, the study did not consider the SSI effects, which was demonstrated significantly influencing the relative responses between adjacent bridge structures (Chouw and Hao 2008). The latter study demonstrated the importance of considering ground motion spatial variations in calculating the relative displacement. As spatial variability of the ground motions at multiple supports of bridge structures are inevitable due to the wave propagation and different soil conditions along the length of the bridge, the existing restrainers design method must be evaluated considering the additional relative motion caused by spatially varying ground motions and SSI to effectively prevent catastrophic unseating failures.

One of the methods presently suggested by bridge design codes to mitigate pounding and unseating damage of bridge girders is to adjust the fundamental frequencies of the adjacent structures as close as possible (Caltrans 2010). It is recommended for all new constructions to adjust the ratio of fundamental period of the adjacent frames to at least 0.7. This provision of the code is proven to mitigate the pounding effects by reducing out-of-phase vibration of the adjacent bridge structures due to the different natural frequencies (DesRoches and Muthukumar 2002). However, the out-of-phase vibration is not only caused by the different natural frequencies of the adjacent bridge components, spatial variations of the ground motions and the characteristics of soil-structure systems also significantly affect the relative displacement response of the adjacent structures as mentioned above (Chouw and Hao 2005, 2008;

Sextos 2003; Bi *et al.* 2011; Li *et al.* 2012). However, no study has considered spatially varying ground motions and SSI on the response of the adjacent structures with restraining devices. In this paper a numerical investigation is carried out to examine the adequacy of the code provision of adjusting the fundamental periods of the adjacent bridge components with unseating restrainers considering uniform and non-uniform ground motions and SSI effects.

This paper extends the previous study by the authors by performing extensive parametric calculations to investigate the influences of the ground motion spatial variations and SSI on the response of bridge structures with cable restrainers. The effects of SSI on the responses of bridges are considered using the frequency independent soil springs and dashpots. To realistically represent the response of the structure, fibre section model capable of considering the spread of inelasticity throughout the entire section is adopted. Parametric analyses are conducted to investigate the effects of spatially varying ground motions, SSI on the response of bridge as well as unseating restrainers at the bridge hinges.

2. MODEL DESCRIPTION

In this study four five-span bridge models are used for the analysis representing two bridge geometries. The expansion joints in the bridge are located nearly at inflection points (i.e., 1/4 to 1/5 of span). The bridge deck consists of box-type girders with pre-stressed concrete. The bridge models are adopted from Feng *et al.* (2000), Kim *et al.* (2003) and are representative of typical Californian bridges. 2-D nonlinear finite element models are used for the analysis, representing a wide variation in ratio of fundamental periods of adjacent structures. Following lists the four bridge models considered in the study:

- Model Bridge 1(a): a five-span bridge with single intermediate expansion joint and equal column height of 19.83 m and diameter 2.44 m.
- Model Bridge 1(b): a five-span bridge with single intermediate expansion joint and equal column height of 19.83 m and the stiffer frame column diameter 3.66 m and the flexible frame column diameter 2.44 m.
- Model Bridge 2(a): a five-span bridge with two intermediate expansion joints and equal column height of 19.83 m and diameter 2.44 m.
- Model Bridge 2(b): a five-span bridge with two intermediate expansion joint and equal column height of 19.83 m and the stiffer central frame column diameter 3.66 m and the flexible frame column diameter 2.44 m.

The geometry, boundary conditions and finite element model of these bridges are shown in Figure 1. The bridge structures are modelled using the nonlinear software package Seismostruct (Seismosoft 2012). Concrete bents are modelled using force based reinforced concrete beam column elements. Reinforced

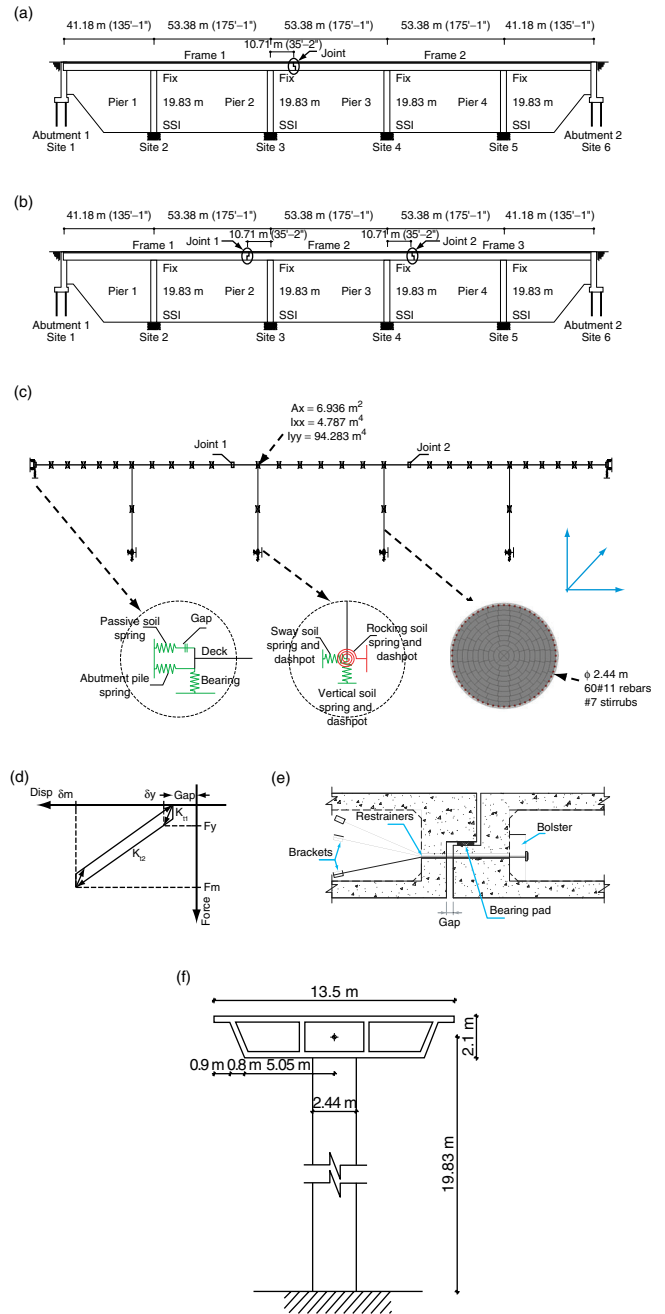


Figure 1. Bridge Models used for the study: (a) Bridge 1 (with a single expansion joint); (b) Bridge 2 (with two expansion joints); (c) finite element model of Bridge 2; (d) analytical model of impact element; (e) typical joint detail; and (f) bridge cross sectional details

concrete sections are constructed from three materials, namely unconfined concrete, confined concrete and reinforcing steel. The unconfined and confined concrete behaviour is modelled using the nonlinear concrete model that follows the constitutive relationship proposed by Mander *et al.* (1988) and the cyclic rules proposed by Martinez-Rueda and Elnashai (1997). The confinement effects provided by the lateral transverse reinforcement are incorporated through the rules proposed by Mander *et al.* (1988), whereby constant confining pressure is assumed throughout the entire stress-strain range. To represent the behaviour of the steel re-bars, Menegotto-Pinto steel model (Menegotto and Pinto 1973) is used. The yield strength of the rebars is 415 MPa, and an elastic modulus, E_s is 200 GPa. The superstructure of the bridge is modelled using elastic beam column elements. As shown in Figure 1(c) each deck is discretised into six elements and each pier, which is modelled using force based beam column element, is subdivided into two elements. Elastomeric bearings at the bridge abutments and bridge joints are modelled using the elastic plastic element. The bridges consist of 6 elastomeric bearing of 0.4 m by 0.3 m area each. The initial stiffness of the elastomeric bearing, K_o , is given by Eqn 1.

$$K_o = \frac{GA}{h_r} \tag{1}$$

where A is the area of the elastomeric bearing, G is the shear modulus of the elastomers and h_r is the thickness of the elastomeric bearing pads. The initial stiffness of each bearing is calculated to be 4.41 kN/mm. The initial stiffness of six bearings is 26.46 kN/mm and coefficient of friction, μ , at the interface of concrete surface and elastomeric bearing is taken as 0.20. The yield force of the bearing is thus calculated to be 498 kN.

2.1. Soil-Structure Interaction (SSI)

SSI at pier base is incorporated using the frequency-independent lumped spring-dashpot systems. The bridge piers analysed in this study rest on the spread footings with size of 7 m x 7 m. In this study dynamic soil stiffness (springs and dashpot) of the foundation are calculated based on the study of Mylonakis *et al.* (2006) using graph and tables for different modes of vibration based on assumption of surface foundation on homogeneous half space. To be compatible with the time-domain nonlinear inelastic analysis framework of the computational platform frequency-independent values are assigned to the foundation impedances

corresponding to a frequency of 1.11 Hz ($T = 0.9$ sec), according to the common assumption of calculating the dynamic impedance matrix based on the predominant frequency range of the input motion. The selected frequency for calculating the foundation impedance is close to the fundamental period of the bridge segments thus would lead to higher responses. Two linear translational and one rotational springs and dashpots are used to represent the stiffness and damping introduced due to SSI. All coefficients of springs and dashpots for sway, vertical and rocking degrees of freedom used to define the soil-foundation model are summarized as follows:

$$K_z = k_z \left(\frac{4.54GB}{1-\nu} \right), \quad C_z = (\rho V_{La} A_b) \hat{c}_z \tag{2}$$

$$K_x = k_x \left(\frac{9GB}{2-\nu} \right), \quad C_x = (\rho V_s A_b) \hat{c}_x \tag{3}$$

$$K_{ry} = k_{ry} \left(\frac{0.45GB^3}{1-\nu} \right), \quad C_{ry} = (\rho V_{La} I_{by}) \hat{c}_{ry} \tag{4}$$

where $K_z, C_z, K_x, C_x, K_{ry}, C_{ry}$ are the vertical stiffness, vertical viscous damping, sway stiffness, sway viscous damping, rocking stiffness and rocking viscous damping, respectively. k_z, k_x, k_{ry} are vertical, sway and rocking dynamic stiffness coefficients. $\hat{c}_z, \hat{c}_x, \hat{c}_{ry}$ are vertical, sway and rocking dynamic dashpot coefficients. B, A_b, I_{by} are the length, area and moment of inertia about the y-axis of the square foundation as shown in Figure 1. G, ρ, ν, V_s and V_{La} are the shear modulus, soil density, Poisson's ratio, shear wave velocity and Lysmer's analog wave velocity, respectively. In this study without losing generality only the local soil site classes presented in Table 1 are considered based on Caltrans (2010) and FEMA

Table 1. Local soil site classes

Site class	Shear wave velocity, V_s (m/s)	Selected value of V_s (m/s)
C. Very dense soil	360–760	400
D. Stiff soil	180–360	220

356 (2000). Soil with shear wave velocity of 400 m/s, Poisson's ratio of 0.4 and density of 19 kN/m³, respectively is adopted for soil site class C. For soil site class D, the shear wave velocity of 220 m/s, Poisson's ratio of 0.4 and soil density of 1.8 kN/m³, respectively is adopted. The elastic shear modulus, G_o , is calculated by following equation (Richart and Whitman 1967).

$$G_o = \left(\frac{\rho V^2}{g} \right) \quad (5)$$

Under seismic shaking the soil behaviour is strongly nonlinear. In this study to approximately include the soil nonlinearity, the reduced shear modulus, G , equal to 67% of the G_o based upon FEMA 356 (2000) is used. To investigate the effects of SSI, the response of bridge on two soil site classes are compared against fixed base cases. The abutments of the bridges on the raised embankments are supported on the pile foundation. The interaction effects at the bridge abutments are modelled using two separate nonlinear springs to model the pile stiffness and passive soil stiffness at abutment. The nonlinear abutment behaviour in this study reflects the design recommendation from Caltrans (Caltrans 2010). The Caltrans recommendation of effective stiffness of 7 kN/mm/pile is used in this study with an ultimate strength of 119 kN/pile. Tri-linear symmetrical models implemented by Choi (2002), which act in both active and passive loading of the abutments, are used to represent the pile stiffness at abutments. 24 piles are present in each abutment. It is assumed that the piles become plastic at a deformation of 25.4 mm, and the first yield occurs at 30% of the ultimate deformation. This corresponds to a yielding force of 70% of ultimate force. Elastic plastic spring with initial stiffness of 28.7 kN/mm/m is used to represent the passive soil stiffness at abutment back-wall (Caltrans 2010). Abutment stiffness and yield capacity can be calculated in SI units as (Caltrans 2010):

$$K_{\text{abut}} = \left(\frac{K_{ai}wh}{1.7} \right) \quad (6)$$

$$P_{bw} = \left(\frac{239A_c h}{1.7} \right) \quad (7)$$

where K_{abut} is the stiffness of an abutment with initial embankment fill stiffness of K_{ai} , effective abutment width of w , and height h . The yield strength of the abutment back wall, P_{bw} can be calculated based on Eqn 7, in which A_e is the effective area of the back wall. For the bridge models considered in the current study, the height and the width of the back wall is 2.25 m and 14.5 m, respectively.

Fundamental period of the bridge segments and the ratio of their fundamental periods are presented in Table 2. The ratios of fundamental natural periods of the fixed bridge models 1(a) and 2(a) are above 0.7 (i.e. $T_i / T_j \geq 0.7$, where T_i and T_j are the natural period of the stiffer and flexible frames, respectively). To investigate response of the bridge segments with distant fundamental frequencies, the diameters of piers of the stiffer frame of the both bridge models are increased by 1.5 times to that of the original model, i.e., stiffness is increased to change its vibration frequency. This resulted in the two new bridge models with the ratio of the natural frequencies lower than 0.7. However, the inclusion of soil spring affects the natural frequencies of the bridge structures. Due to the flexibility introduced by the soil springs the natural period of the bridge structures increases and the ratio of the periods of the adjacent frames with soil springs shifts closer to unity.

2.2. Impact Element

It is recognized that pounding between adjacent bridge decks during strong earthquake shaking can affect the bridge response. Pounding resulting from the out-of-phase motion of the adjacent bridge structures could result in damages at the joints and may even result in

Table 2. Fundamental periods of model bridges

Bridge model	Stiff frame period (T_i , sec)	Flexible frame period (T_j , sec)	Period ratio (T_i/T_j)
Model 1a (Fixed base)	0.84 (Frame 1)	0.92 (Frame 2)	0.91
Model 1b (Fixed base)	0.55 (Frame 1)	0.92 (Frame 2)	0.60
Model 2a (Fixed base)	1.00 (Frame 2)	1.25 (Frame 1 & 3)	0.72
Model 2b (Fixed base)	0.88 (Frame 2)	1.25 (Frame 1 & 3)	0.50

unseating of the adjacent spans. Hence it is essential to include the effects of pounding in the numerical model. This can be done in finite element model by using a gap element to monitor the relative displacement between the adjacent sections of the bridge. Once the closing relative displacement is larger or equal to the associated gap pounding occurs. The concept of the gap element is quite simple. However, actual modelling of pounding behaviour can be quite cumbersome. Linear impact model which has been widely adopted to model the pounding between adjacent structures has a limitation of not allowing energy dissipation and thus may overestimate the system response due to the impact. The impact model such as Kelvin, Hertz damp model etc., which considers the energy dissipation during the pounding, is difficult to implement in nonlinear software packages. Muthukumar (2003) recommended a simplified bilinear spring model to capture the effects of impact including the energy dissipation. The impact model is an approximate representation of the Hertz damp model (Muthukumar and DesRoches 2006). In this study the impact model proposed by Muthukumar (2003) is used to represent the contact and pounding during the seismic event. Figure 1(d) shows the typical representation of the bilinear spring model used to model pounding. In this study the maximum deformation or penetration δ_m is assumed to be 25.4 mm and δ_y is assumed to be 0.10 (δ_m). The coefficient of restitution, e is assumed to be 0.8. The K_{r1} and K_{r2} are calculated to be 10.68 GN/m and 3.68 GN/m respectively. More details on determination of these pounding parameters can be found in Muthukumar (2003). In this study, without losing generality the gap length of the internal expansion joints is assumed to be 25 mm and that between abutment and deck is assumed to be 50 mm.

3. GROUND MOTION MODELLING

It is common in engineering practice to simulate spatially varying ground motions that are compatible with the specific design response spectra. Many stochastic ground motion simulation methods have been proposed by different researchers. For example, Hao *et al.* (1989) and Deodatis (1996) simulated the spatially varying ground motions in two steps: first the spatially varying ground motion time histories are generated using an arbitrary power spectral density function, and then adjusted through iterations to match the target response spectrum. Usually a few iterations are needed to achieve a reasonably good match. More recently, Bi and Hao (2012) further developed this method by simulating the spatially varying ground motions which are compatible with the ground motion power spectral

densities that are related to the target design response spectra instead of arbitrary power spectral density functions. Compared with the methods suggested by Hao *et al.* (1989) and Deodatis (1996), less or even no iterations are needed in the latter approach (Bi and Hao 2012), the latter method is thus computationally more efficient. The method proposed by Bi and Hao (2012) is adopted in the present study to simulate the spatially varying ground motion time histories that are compatible with the design spectra specified in the Japanese Highway Code (2004). The acceleration response spectrum of a Type II ground motions, which represent the ground motion generated by inland earthquake at short distance (Near-fault), developed by smoothing the response spectra that are computed from the ground motion records obtained in the 1995 Kobe earthquake is used in this study. The spatially varying ground motions for group 2 sites, i.e., the medium soil site conditions, are simulated. In the simulations, the sampling and upper cut-off frequencies were set to 100 and 25 Hz, respectively, and the duration of 40.95 s is selected to have a convenient total number of points (4096) for a fast Fourier transform.

The spatial variation properties between ground motions recorded at two locations j and k on ground surface is modelled by a theoretical coherency loss function (Sobczyk 1991).

$$\begin{aligned} \gamma_{jk}(i\omega) &= |\gamma_{jk}(i\omega)| \exp(-i\omega d_{jk} \cos \alpha / v_{app}) \\ &= \exp(-\beta \omega d_{jk}^2 / v_{app}) \times \exp(-i\omega d_{jk} \cos \alpha / v_{app}) \end{aligned} \quad (8)$$

where β is a constant reflecting the level of coherency loss. In order to gain the wider perspective on the response variation due to the non-uniform ground motions, simulation of the ground motions is carried out for three levels of coherency losses, i.e., $\beta = 0.0005$, 0.0010 and 0.0015 are used in the study to represent highly, intermediately and weakly correlated ground motions respectively. To obtain relatively unbiased structural responses, 3 sets of ground motion time histories are simulated for each coherency loss levels. d_{jk} is the distance between the two locations j and k in the wave propagation direction, f is the frequency in Hz, v_{app} is the apparent wave velocity, and α is the seismic wave incident angle. In the present study, v_{app} is assumed to be 400 m/s, and $\alpha = 60^\circ$. The values of v_{app} selected is realistic for typical highway bridge sites in California in consideration of the measured shear wave velocities, such as the Painter street bridge and Meloland Road Overcrossing (Zhang and Markis 2002a, b). The same value of v_{app} has been adopted in previous studies for Californian bridges (Huo and

Zhang 2013). It is to be noted that the bridge models used in the analysis are 2D models and the spatially varying ground motions are only applied along the longitudinal direction (X-axis) of the bridge (Figure 1(c)). Vertical ground motion is not considered because it has relatively insignificant effect on relative displacement at joints between adjacent bridge structures.

Figure 2 compares the response spectra of the simulated ground motions and the target design spectra at the 6 sites shown in Figure 1. It shows that the response spectrum of the simulated ground motions match well with the target design spectrum for the respective site. Figure 3 shows the comparison of the empirical coherency loss function (Eqn 8) between site 1 and other sites and the corresponding values of the simulated motions. Good match can also

be observed except for $|\gamma_{15}|$ and $|\gamma_{16}|$ in the high frequency range. This, however, is expected because as the distance increases, the cross correlation between the spatial motions or their coherency values decrease rapidly with the frequency. Previous studies (Hao *et al.* 1989) revealed that the coherency value of about 0.3–0.4 is the threshold of cross correlation between two time histories because numerical calculations of coherency function between any two white noise series result in a value of about 0.3–0.4. Therefore, the calculated coherency loss between two simulated time histories remains at about 0.4 even the model coherency function decreases below this threshold value. It should be noted that the simulated coherency losses between ground motions at other locations, which are not shown here, also match the models well.

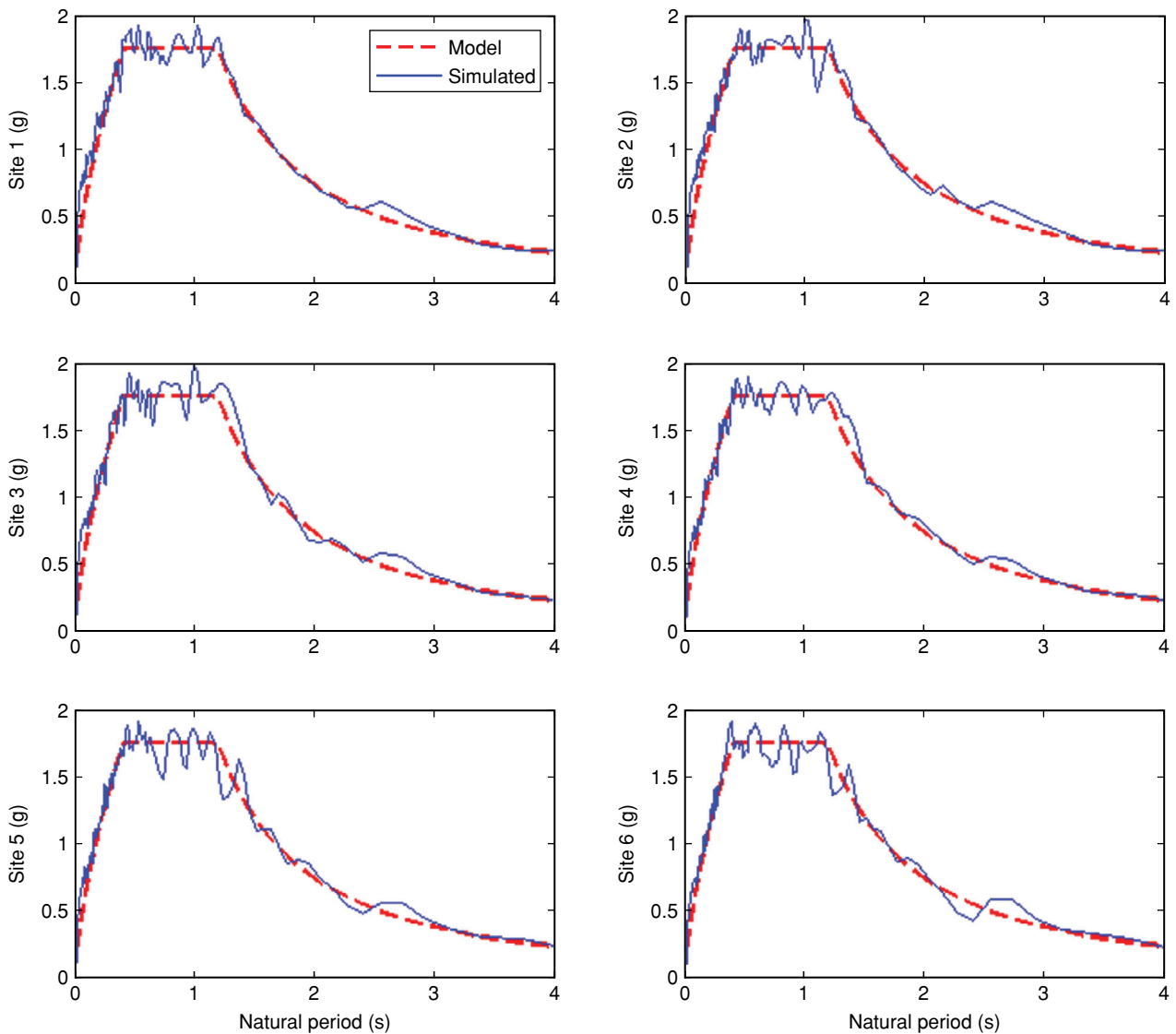


Figure 2. Comparison of the response spectra of simulated ground motions with the target spectrum

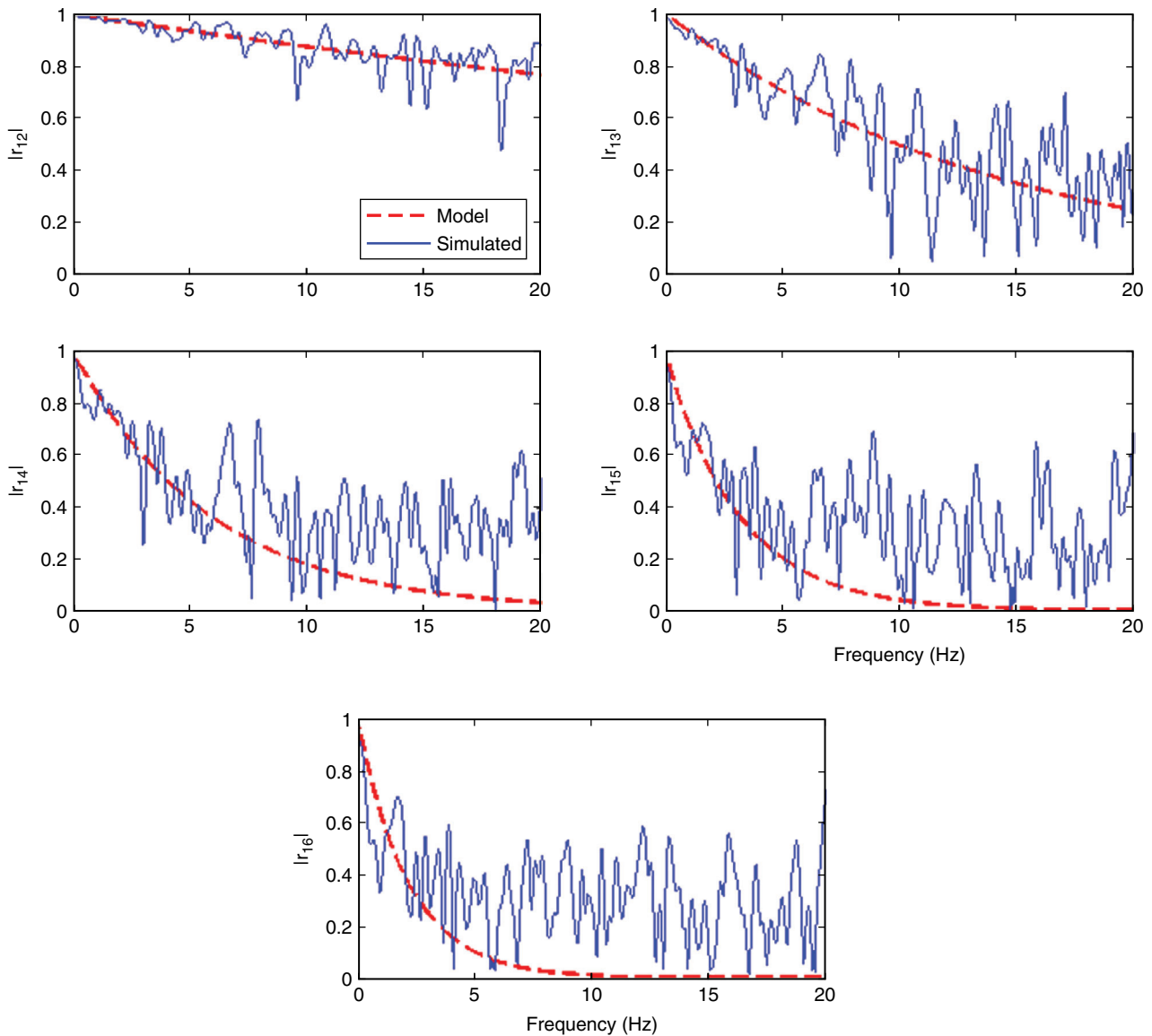


Figure 3. Coherency losses of simulated ground motions

4. RESTRAINER DESIGN AND MODELLING

In this paper a widely used restrainer design method proposed by DesRoches and Fenves (2000) is evaluated to identify its adequacy to prevent unseating damage of bridge decks subjected to spatially varying ground motions. The method, developed to predict the restrainer stiffness required to limit the hinge movement to a certain acceptable limit subjected to uniform ground motion, is briefly discussed here. The method is based on the analysis of a two-degree-of-freedom system as shown in Figure 4 (a), representing the fundamental vibration mode of adjacent bridge frames. The relative hinge displacement, D_{eq} , is estimated by combining the modal response using the complete quadratic combination (CQC) rule (Der Kiureghain 1980):

$$D_{eq} = \sqrt{D_1^2 + D_2^2 - 2\rho_{12}D_1D_2} \quad (9)$$

where D_1 and D_2 are modal displacements and ρ_{12} is the correlation coefficient between the response of the two modes defined as:

$$\rho_{12} = \frac{8\sqrt{\xi_1\xi_2}(\xi_1 + \beta\xi_2)\beta^{3/2}}{(1 - \beta^2)^2 + 4\xi_1\xi_2\beta(1 + \beta^2) + 4(\xi_1^2 + \xi_2^2)\beta^2} \quad (10)$$

where β is the ratio of the frame fundamental periods, T_2/T_1 , and ξ_1 and ξ_2 are the corresponding modal damping ratios. The main design parameters are the frame stiffness, masses, ductility demand and allowable hinge displacement. The schematic view of relative

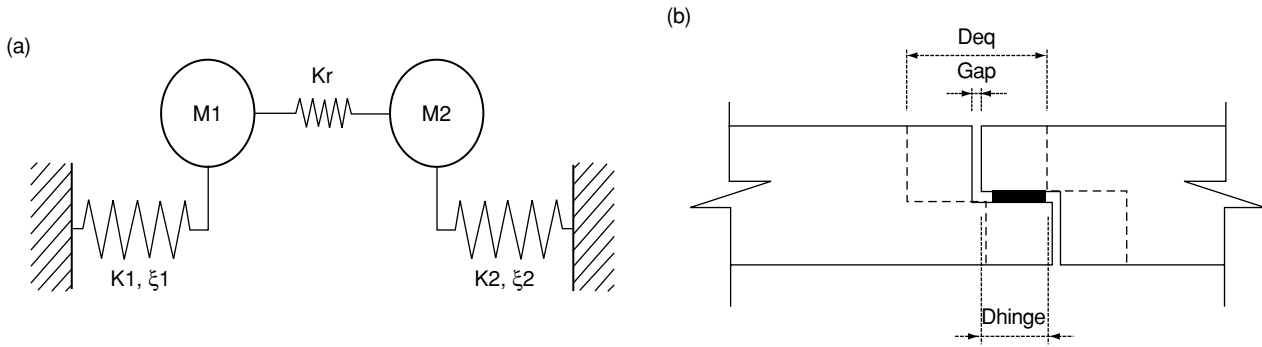


Figure 4. (a) Linearized analytical model of the hinge; and (b) Bridge intermediate hinge

displacement at the bridge expansion joint during an earthquake event is shown in Figure 4(b), where D_{eq} represents the Maximum Relative Hinge Displacement (MRHD) that could be expected during the seismic event and D_{hinge} is the available hinge seat width. The allowable hinge displacement, D_r , is calculated by subtracting the minimum required bearing length, D_b which is required for spans to remain seated without losing the functionality of the bridge, from the available seat width, D_{hinge} . The target yield displacement of the restrainers, D_y , is the difference between the allowable hinge displacement, D_r and the restrainer slack, D_s . Using D_{eq} , the restrainer stiffness, Kr , needed to limit the hinge displacement to D_r is determined from the sensitivity of the hinge displacement to the restrainer stiffness:

$$\frac{\delta D_{eq}}{\delta Kr} = -\frac{1}{Km + Kr} D_{eq} \tag{11}$$

where $1/Km = 1/K_1 + 1/K_2$ is the sum of the flexibilities of the two frames. Performing a Taylor series expansion about the current estimate of the hinge displacement, Deq_j , and solving for an improved estimate of the restrainer stiffness at the next step, Kr_{j+1} , gives

$$Kr_{j+1} = Kr_j + (Km + Kr_j) \frac{(Deq_j - Dr)}{Deq_j} \tag{12}$$

Each iteration of the procedure consists of a 2-DOF modal analysis for D_{eq} , followed by the use of the updated estimate of restrainer stiffness. The yielding behaviour of ductile frames is accounted for in the restrainer design procedure by determining an equivalent stiffness and damping ratio based on the maximum displacement of the frames (Gulkan and Sozen 1974). A typical case requires three to five iterations to

converge. Parametric studies and case studies showed that the procedure limits the relative hinge displacement to a specified value for a wide range of bridges subjected to uniform ground motions (DesRoches and Fenves 2000).

In this study available hinge seat width, D_{hinge} , is taken as 200 mm, which represents narrow seated bridges of San Fernando earthquake era. The restrainer slack, D_s , is assumed to be 25 mm. Minimum required bearing length, D_b is assumed 87 mm. The target yield displacement, D_y , of the restrainer is thus calculated to be 88 mm. Letting D_y be the same as the yield displacement of restrainers at 1.75% strain (DesRoches and Fenves 2000); the restrainer length is calculated to be 5.04 m. The stiffness of the restrainers required to restrict the hinge movement to the prescribed value, i.e., $D_r = 113$ mm, is determined using the modal analysis with multiple trials.

Typical 19 mm diameter high-strength cable used in Caltrans bridges with cross sectional area of 143 mm² and the yield strength of 1210 MPa are used in this study. The numbers of restrainers required to limit the hinge opening subjected to design earthquake motion calculated for bridge model 1(a) and model 2(a) are 2 and 8, respectively. In this study, without losing generality a practical number of 10 restrainers are provided for each bridge model at each joint, implying slight over design of the required cable restrainers. It is assumed that the connection between the deck and the restrainers are strong so that all the deformation will concentrate on the restrainers.

The drawback of the above method is that it only considers the relative displacement induced due to the different fundamental periods of the adjacent structures. That is why it predicts only 2 restrainers are required when the adjacent bridge frames have close vibration frequencies. It neglects the influences of spatial variation of ground motion, which results in further out-of-phase vibration, thus could

underestimate the relative displacement between the structures. This underestimation of the relative displacement could significantly affect the required stiffness and strength of the restrainers. As spatial variation of the ground motions are unavoidable and the failure of the restrainers could lead to the unseating of the bridge spans, it is essential to evaluate the effectiveness of the method by including the effects of ground motion spatial variations.

In numerical simulations the restrainers are modelled using two node truss elements with tension only behaviour. The slack of 25 mm is provided to accommodate the thermal movement of the deck. Bilinear force-displacement relationship is used to model the constitutive behaviour of the restrainers. As the restrainers are designed considering only the uniform ground motions, which might significantly underestimate the relative joint displacements, it is likely that restrainers will be significantly stressed and may even get fractured. Therefore, the failure of the restrainers is taken into account and the ultimate strain of the restrainers is taken as 4.50%. Once the ultimate strain capacity is reached the adjacent span can separate freely without any restriction provided by the restrainers. The hysteretic behaviour of the restrainer is presented in Figure 5.

5. EFFECTS OF SPATIAL VARIATION OF GROUND MOTION

5.1. Wave Passage Effect

One of the sources for the variation of the ground motion at different bridge supports is the travelling seismic wave. Wave passage effect is primarily described by the apparent wave passage velocity, v_{app} , which depends on incident angle of seismic waves into the site and the site condition. A study of the recorded

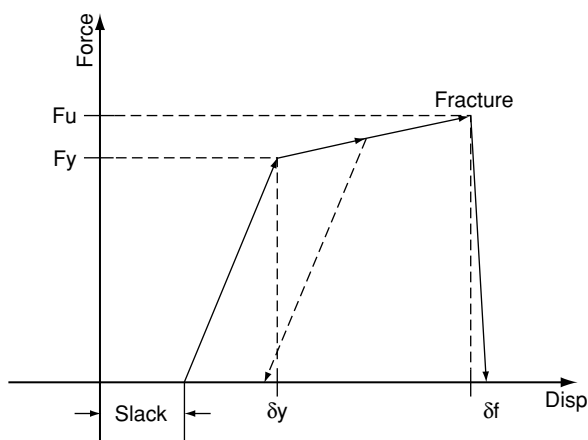


Figure 5. Hysteretic behaviour of steel restrainers

time histories revealed that the apparent wave velocity is frequency dependent and quite irregular in nature (Hao *et al.* 1989). To consider the randomness of the apparent wave velocity three different values (i.e. 400, 800, 1600 m/s) of wave velocity is considered in this study. Ground motion simulated for site 1 is used in the analysis with appropriate time delays to represent the wave passage effect. Without losing the generality, only the responses of the bridges on soil site C ($V_s = 400$ m/s) is presented. Bridge structure responses to the three independent sets of simulated spatially varying ground motions are analysed, and the average responses are calculated and discussed. In order to quantify the effects of spatially varying ground motions normalized values of response are used. The normalised value is defined as below;

$$\text{Normalised value} = \frac{\text{Average response to spatially varying ground motions}}{\text{Average response to uniform ground motion}} \quad (13)$$

Figures 6(a) and 6(b) present comparison of the normalized average drift subjected to the three sets of simulated ground motions for Pier 2 and Pier 3 of bridge model 1(a), respectively. As shown, spatially varying ground motions due to wave passage effect result in reductions in the seismic demand for piers of both the stiff and flexible frames. This is because, as shown in Figure 7, spatially varying ground motions result in more frequent and severe pounding between the adjacent girders and between the girder and abutments. This impedes displacements of bridge frames, because pounding restrain movements of adjacent structures. However, differential support motions adversely influence the relative displacement responses. Normalised Maximum Relative Hinge Displacement (MRHD) and normalised Restrainer Deformation (RD) at intermediate hinges, as presented in Figures 8(a) and 8(b), are significantly increased due to the ground motion spatial variations caused by wave passage effect. Generally speaking, smaller apparent wave velocity results in larger MRHD and RD. For comparison, the deformations when the restrainer yield and fracture are also presented in the figure. As shown for a set of spatial ground motion with the apparent wave velocity 400 m/s the restrainer get fractured and cannot restrain the bridge structures anymore. It should be noted the allowable hinge displacement, D_{hinge} , plotted in Figure 8 (a) is only for the indicative purpose and the unseating of the bridges is not explicitly modelled.

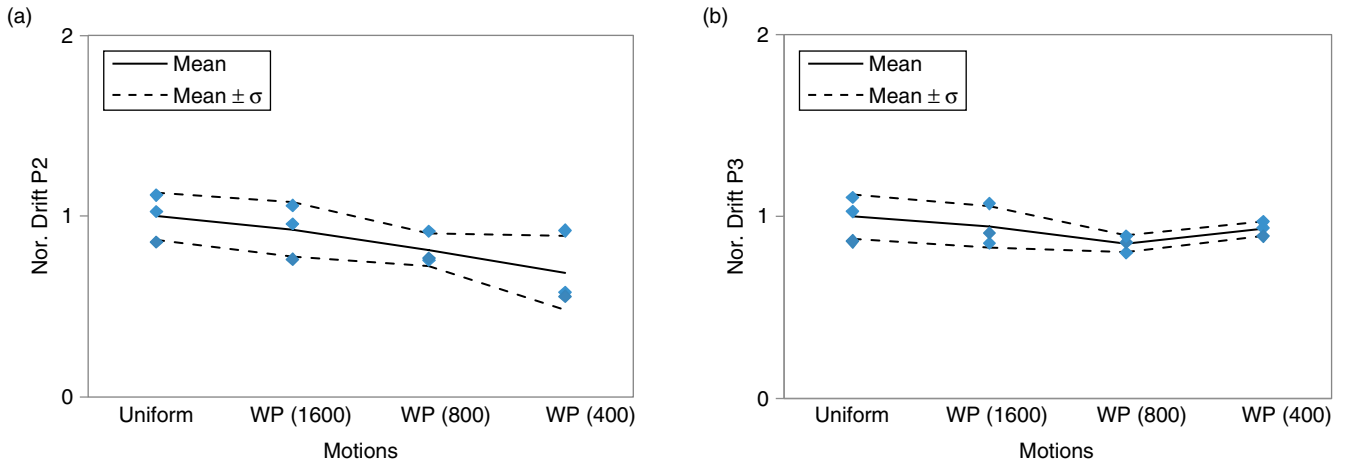


Figure 6. Normalised drift of (a) Pier 2; (b) Pier 3 of bridge 1(a)

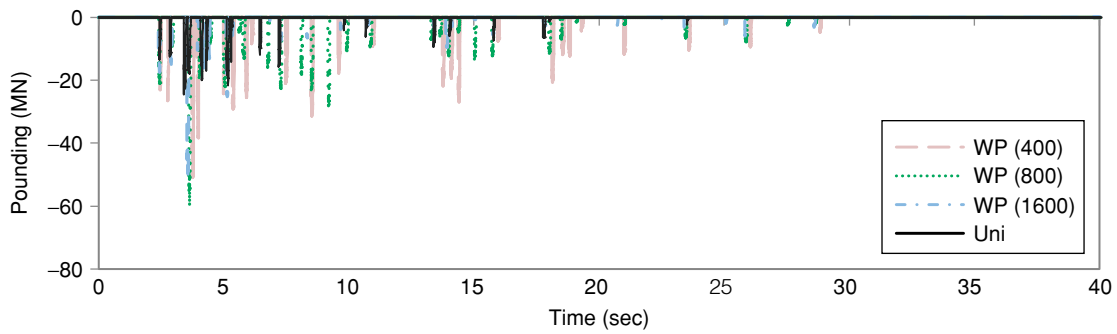


Figure 7. Pounding forces at intermediate hinge of bridge 1(a)

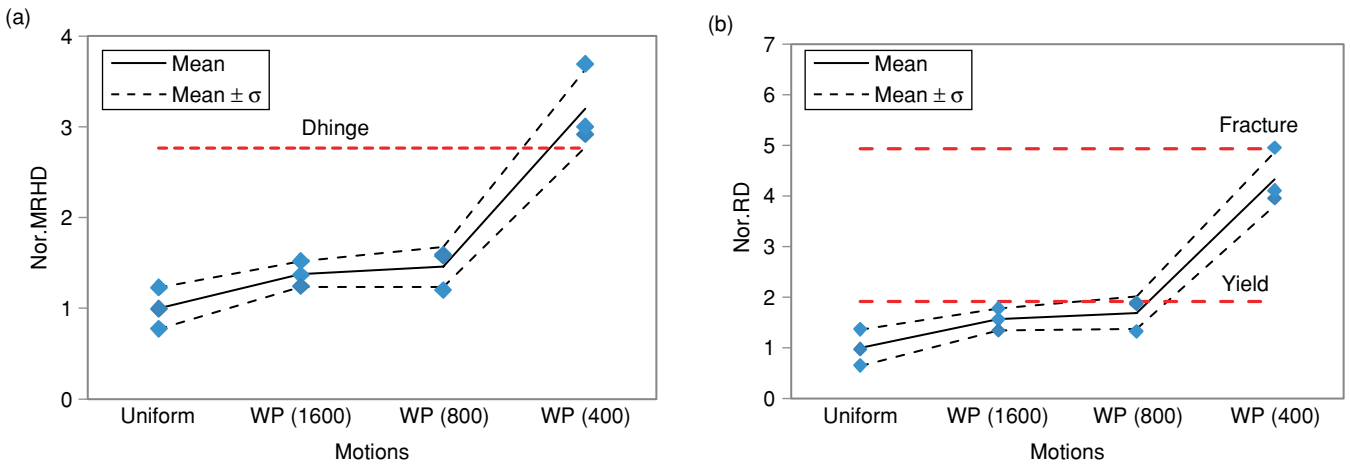


Figure 8. (a) Normalised MRHD; and (b) Normalised RD for bridge 1(a)

5.2. Coherency Loss

Effects of the coherency losses between the ground motions at different bridge supports on the response of bridge structures are parametrically evaluated for three different coherency loss levels as discussed previously. Figures 9(a) and 9(b) presents the comparison of normalised MRHD and normalised RD for spatial

ground motions with different levels of coherency losses and uniform ground motion, respectively. In the figure WP (400) represents the ground motions considering the wave passage effect with apparent wave passage velocity of 400 m/s. CH (Hig), CH (Int) and CH (Wea) represent the cases with highly coherent, intermediately coherent and weakly coherent motions,

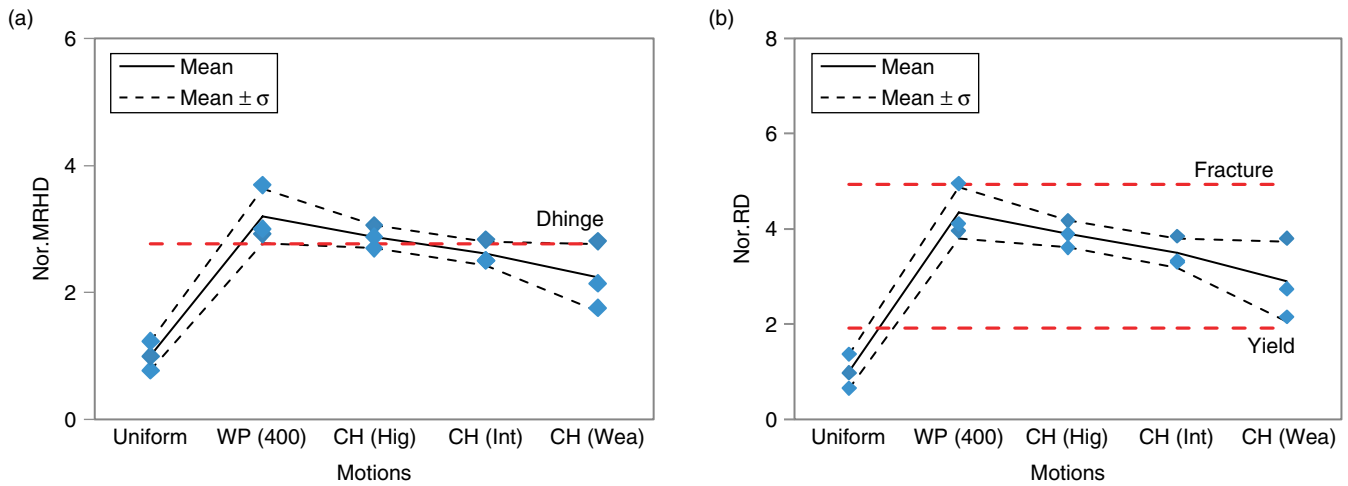


Figure 9. (a) Normalised MRHD; and (b) Normalised restrainers deformation of bridge 1(a)

respectively and have apparent wave passage velocity of 400 m/s. As shown, the largest relative displacement response at the intermediate hinge corresponds to the case considering wave passage effects only. Inclusions of the coherency losses of spatially varying ground motion in fact have beneficial effects on relative responses between the adjacent components of the studied bridge. However, the normalised MRHD for all the cases of spatially varying ground motions are significantly higher than that from the uniform ground motions. As presented in Figure 9(b), the restrainers yielded for all the ground motions except the uniform motions indicating the restrainers designs based on uniform ground motion assumption are inadequate. In a case of spatial ground motion considering only the wave passage effect the relative displacement is large enough to fracture the restrainers, which led to unrestrained movement of the adjacent spans. Figures 10(a) and

10(b) present the normalised MRHD and normalised RD for joint 2 of bridge model 2(a). In this case, however, the spatially varying ground motions considering coherency losses resulted in higher relative displacement. These results indicate that the effects of the coherency losses on the response of the bridge structures are not only dependent upon the ground motions, but also on the bridge geometry. Considering only the wave passage effects of the ground motion spatial variations may lead to inaccurate predictions of bridge structural responses. Uniform excitation assumption significantly underestimates the MRHD and RD. The restrainers designed for uniform ground motion assumption may lose its functionality due to yielding or may even get fractured due to the large relative displacement caused by ground motion spatial variations.

Figures 11(a) and 11(b) show response of Pier 2 and Pier 3 of the bridge model 1(a) subjected to uniform and

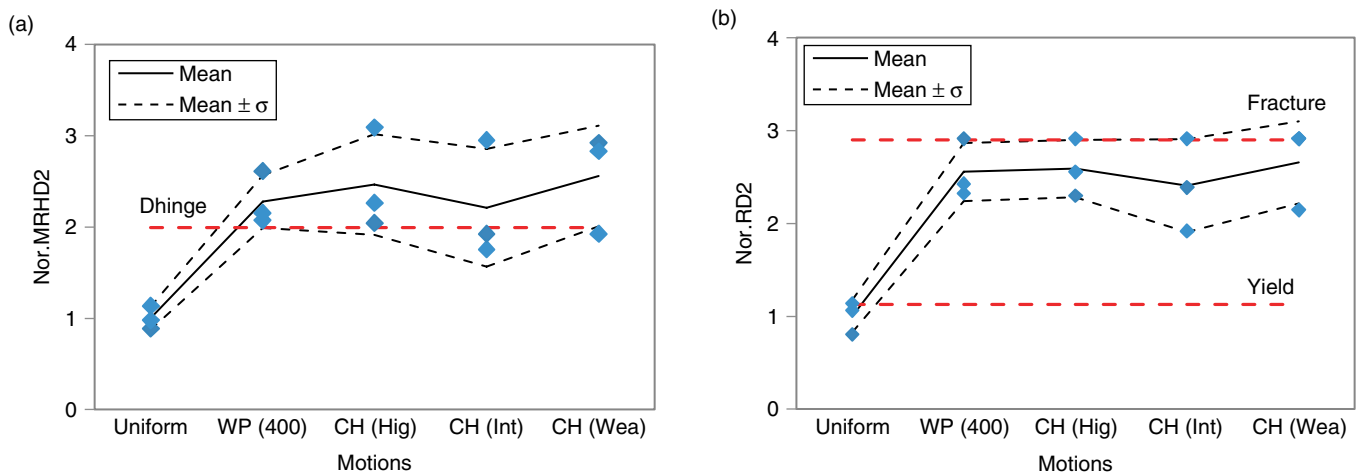


Figure 10. (a) Normalised MRHD; and (b) Normalised RD at joint 2 of bridge 2(a)

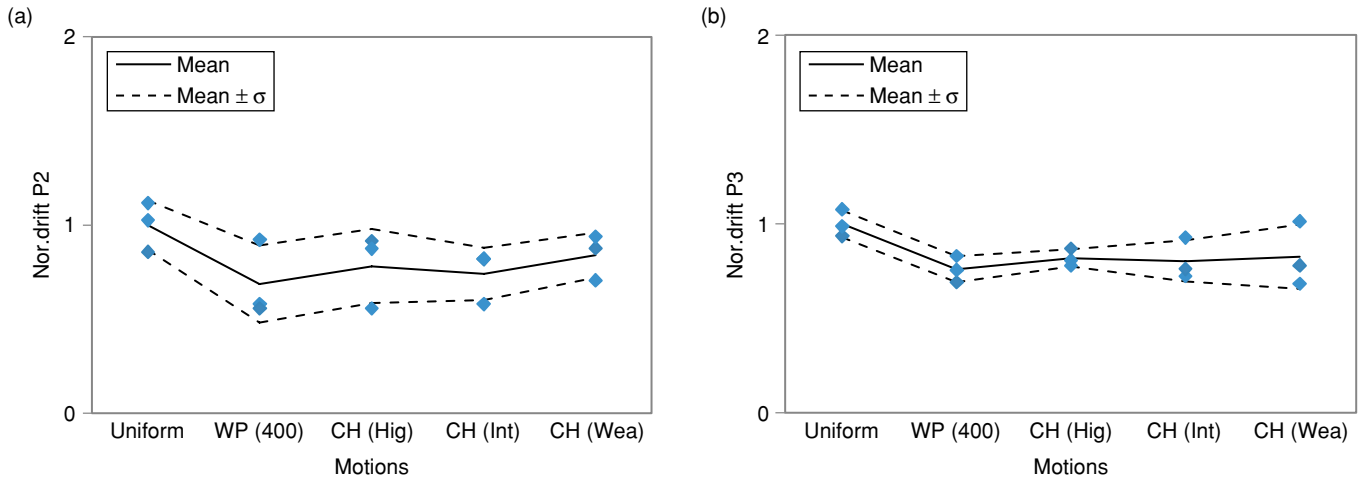


Figure 11. (a) Normalised peak Drift of Pier 2; and (b) Pier 3 of bridge 1(a)

spatially varying ground motions. The results show again that pier drift are reduced due to spatially varying ground motion compared to uniform ground motions. Figures 12(a) and 12(b) present the normalised peak pounding forces for the bridge model 2(a) at joint 1 and joint 2, respectively. As shown the spatial variation of ground motions increases out-of-phase motion between adjacent bridge components. This leads to amplification of peak pounding forces.

6. EFFECTS OF FRAME PERIOD RATIO

To investigate the influence of the spatially varying motions on the relative response of the adjacent bridge frames with close and different fundamental periods, a parametric study is conducted on four bridge models. Bridge codes such as Caltrans (2010) recommend constructing the adjacent structures with close fundamental periods. However, there still lacks

investigations on its effectiveness on the bridges subjected to spatially varying ground motions including the SSI effect. In this study the two bridge model 1(a) and 2(a) with close fundamental periods are compared against bridge models 1(b) and 2(b) with distant fundamental periods. In this case also the bridge model including the SSI for soil class C is discussed. The response of the structures to uniform motion, motion considering wave passage effect only and spatially varying motion considering intermediate coherency losses are investigated. Figures 13(a) and 13(b) present the comparison of MRHD and peak pounding forces for bridge model 1(a) and 1(b). Figures 14(a) to 14(d) compare the pounding forces and relative opening displacement at the two joints of the bridge model 2(a) and 2(b). The results show that code provision of adjusting the fundamental frequencies of the adjacent bridge component close to each other is an effective method to

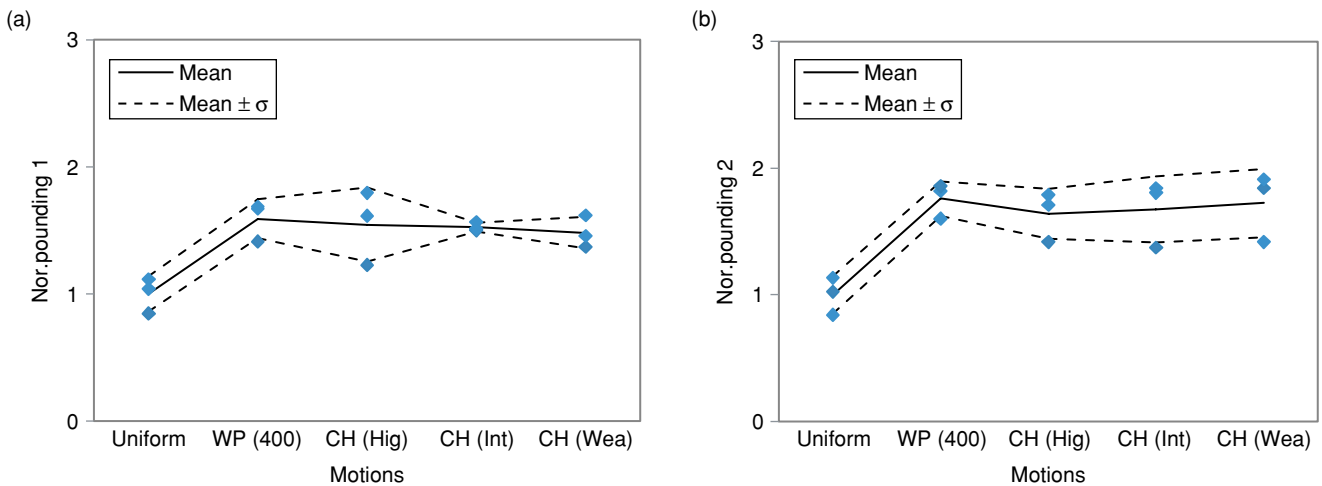


Figure 12. Normalised pounding force at: (a) joint 1; and (b) at joint 2 of bridge 2(a)

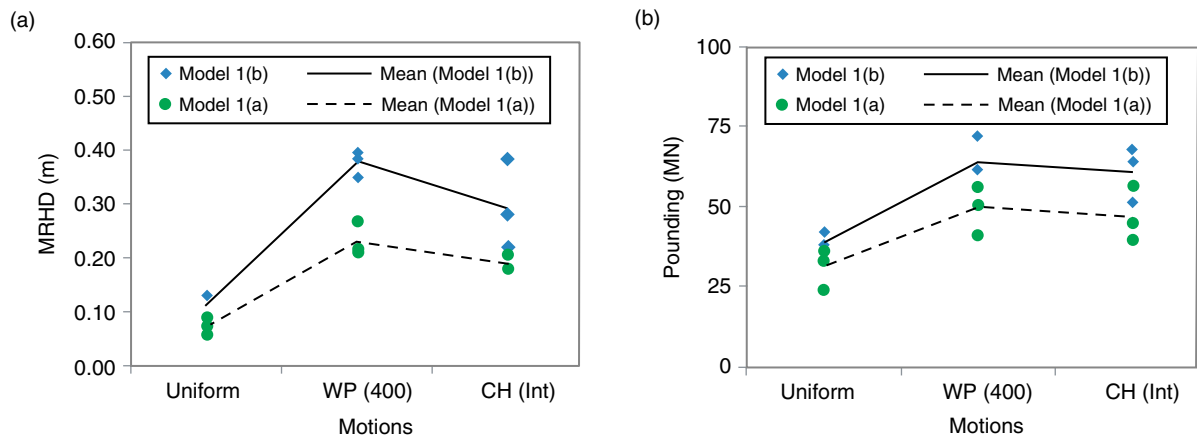


Figure 13. Comparison of: (a) MRHD; (b) peak pounding forces for bridge models 1(a) and 1(b)

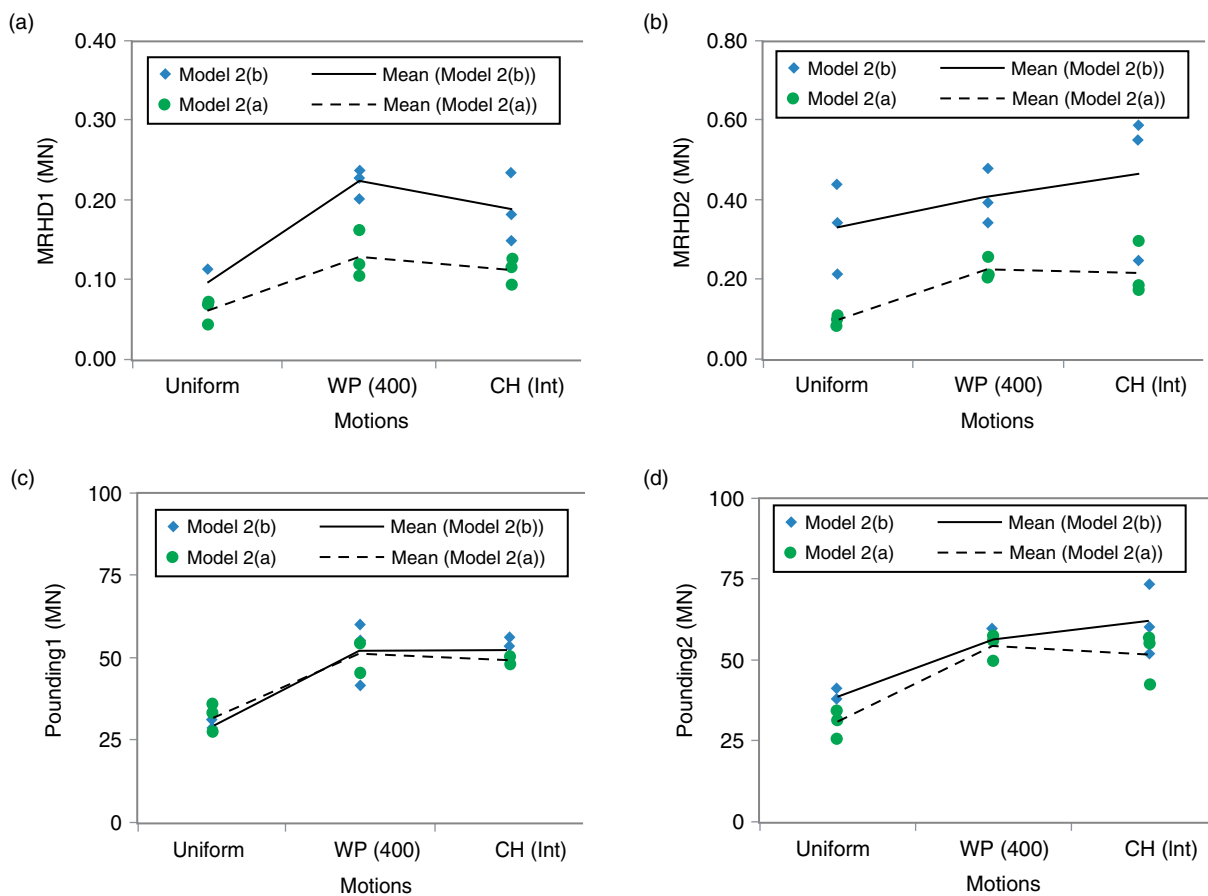


Figure 14. Comparison of: (a) MRHD; (b) peak pounding forces at Joint 1; (c) MRHD; and (d) peak pounding forces at joint 2 of bridge models 2(a) and 2(b)

mitigate pounding forces and relative displacement on bridges under influence of spatially varying ground motions as well. Pounding forces and relative joint opening for bridges with close fundamental periods are significantly lower compared to the bridge with distant fundamental periods. Hence, the code provision of adjusting the fundamental periods of adjacent structures close to each other is justifiable. However, as shown in

Figures 13 and 14, only this might not be sufficient to prevent the bridge structures from relative displacement induced damages caused by spatially varying ground motions. Though the relative displacement and pounding forces are reduced, spatially varying ground motions still results in relative displacements large enough to induce some damages at bridge joints even for the bridges with relatively close fundamental periods.

7. EFFECTS OF SSI

The interaction of the foundation with the surrounding soil and the structures could lead to a very complex and case dependent dynamic response. In this study to identify the influence of SSI on the seismic responses of the bridge a comparative study of the bridges with fixed base and with SSI (for two different soil site conditions) subjected to uniform and spatially varying ground motions are carried out. Figures 15(a) and 15 (b) present the MRHD and the RD at intermediate hinge of bridge model 1(a). As presented, inclusion of SSI reduces the relative displacement response of the adjacent bridge structures. This is because, as presented in Figure 16,

vibration period of the structures increases when SSI is considered. Due to this shift in the fundamental vibration period, the ratio of the periods of the adjacent structures shifts closer to the unity. Hence, the adjacent frames tend to vibrate more in-phase, which in turn reduces the relative displacement between the frames. Similar results were also observed by the previous authors (Chouw and Hao 2003). The SSI, however, has detrimental effect on the relative displacement at abutment joints as shown in Figure 17(a). The period elongation of the adjacent frames due to the SSI results in an increase in out-of-phase motions with stiffer abutments. This causes an increase in relative

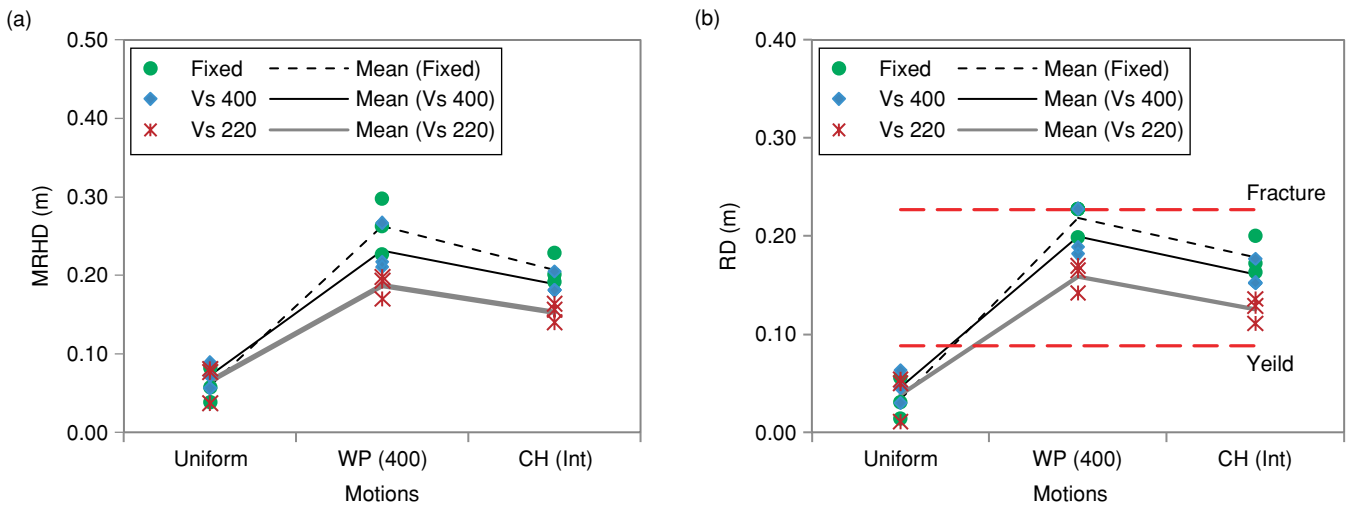


Figure 15. Influence of SSI on: (a) MRHD; and (b) RD at in-span hinge of bridge model 1(a)

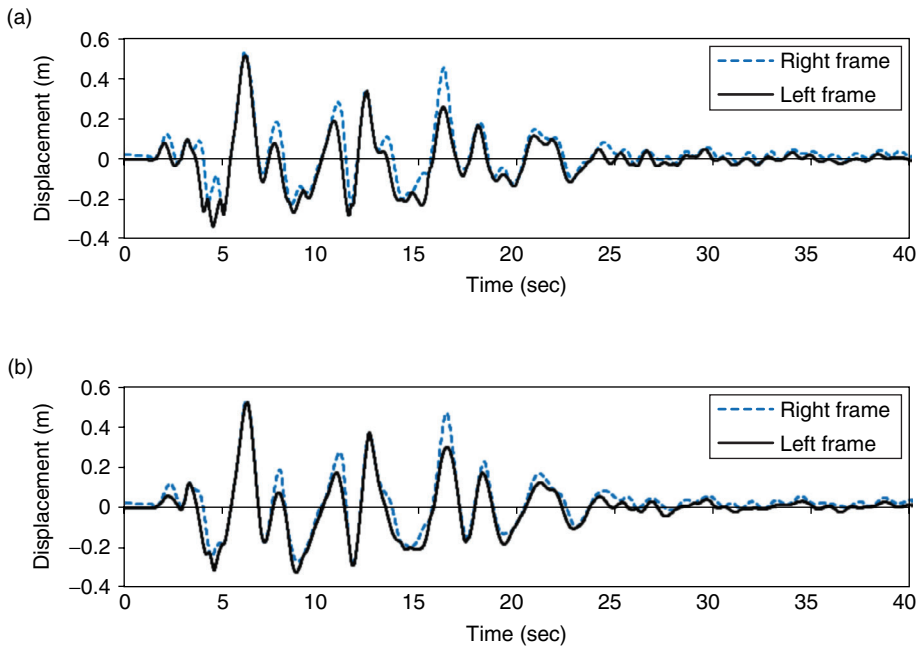


Figure 16. Displacement time-history of bridges girders for: (a) fixed foundation; and (b) with SSI (Vs 220) subjected to spatially varying ground motion

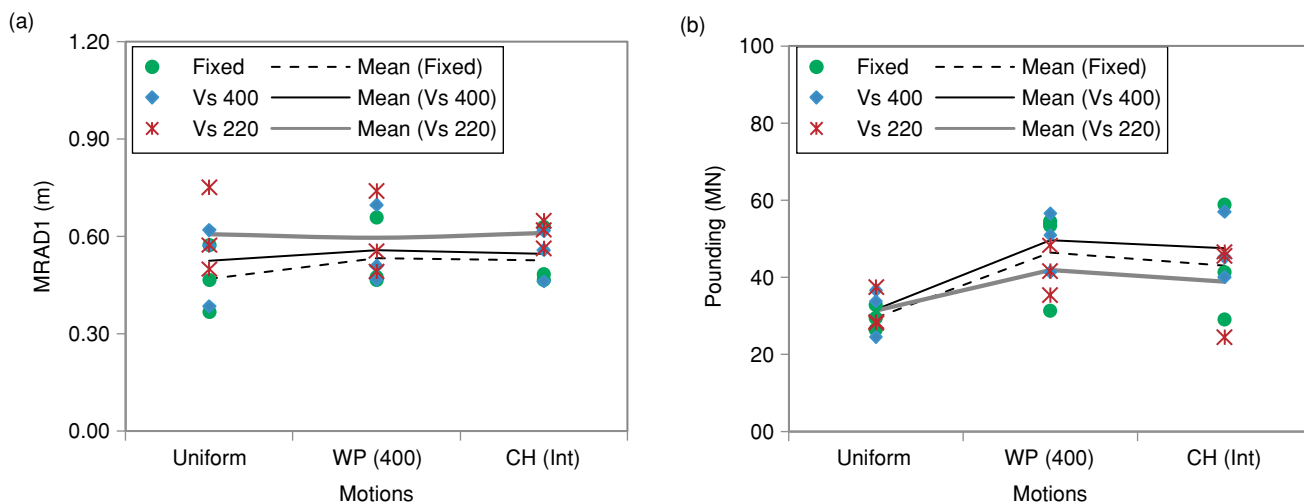


Figure 17. Influence of SSI on: (a) MRAD 1; and (b) Peak pounding force at the internal joint

displacement at both abutments joints. Figure 17(b) presents the peak pounding responses at intermediate joint of the bridge. As shown the pounding response of the adjacent bridge structure is dependent upon the soil site type considered. Pounding forces on the bridge joints with SSI considering soil site class C are always higher compared to the fixed base condition. However, the pounding force for the bridge in softer soil (site class D, $V_s = 220$ m/s) is lower compared to the fixed base condition, except for the uniform ground motions. The results presented highlight that the effects of SSI on the pounding response of adjacent bridge structure is case dependent and it is difficult to generalize the results based on the limited cases considered in the present study. However, the present simulation results demonstrate the importance of considering the SSI effect in bridge response calculations.

Figures 18(a) and 18(b) compare the drift of pier 2 and pier 3 of bridge model 1(a). As shown, inclusion of SSI increases overall displacements of both frames. It is interesting to note that considering SSI reduces the relative displacement (as shown in Figure 15) but increases the drift of both the frames. The softer the soil, the more will be the drift of the frames. However, the relative displacements at intermediate joints are reduced. In order to find out the effects of SSI on the response of the bridge piers, section curvature demand at the top and the base of the bridge piers are compared. Figures 19(a) and 19(b) present the section curvatures of the base of pier 2 and pier 3 of bridge model 1 (a), respectively. The results show that the inclusion of SSI reduces the curvature demand at the base of the pier. However, as presented in Figures 20(a) and 20(b), larger displacements caused by the

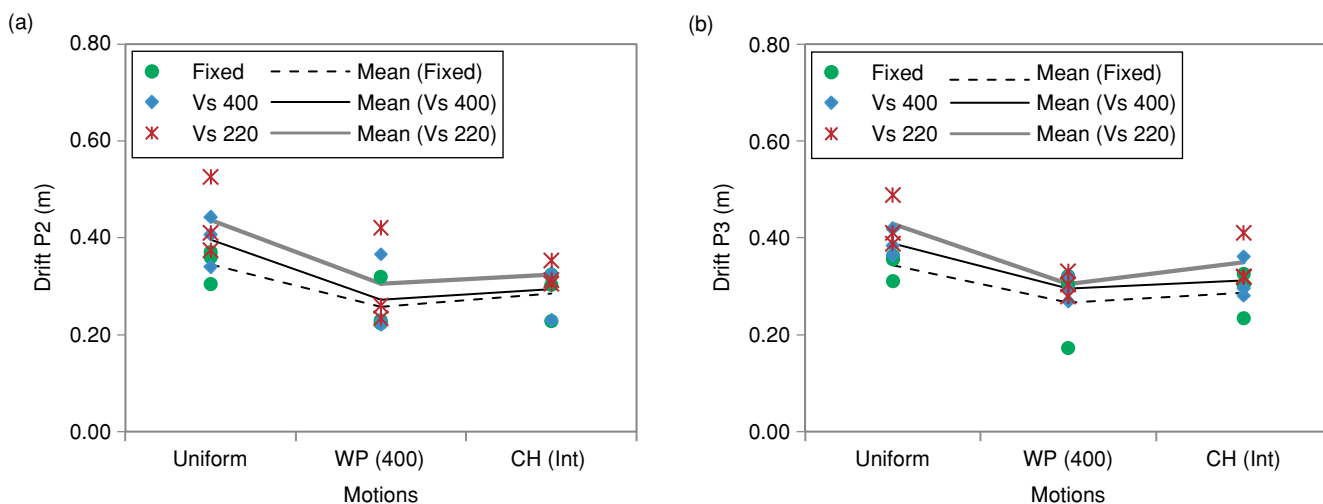


Figure 18. Influence of SSI on the drift of: (a) pier 2; and (b) pier 3

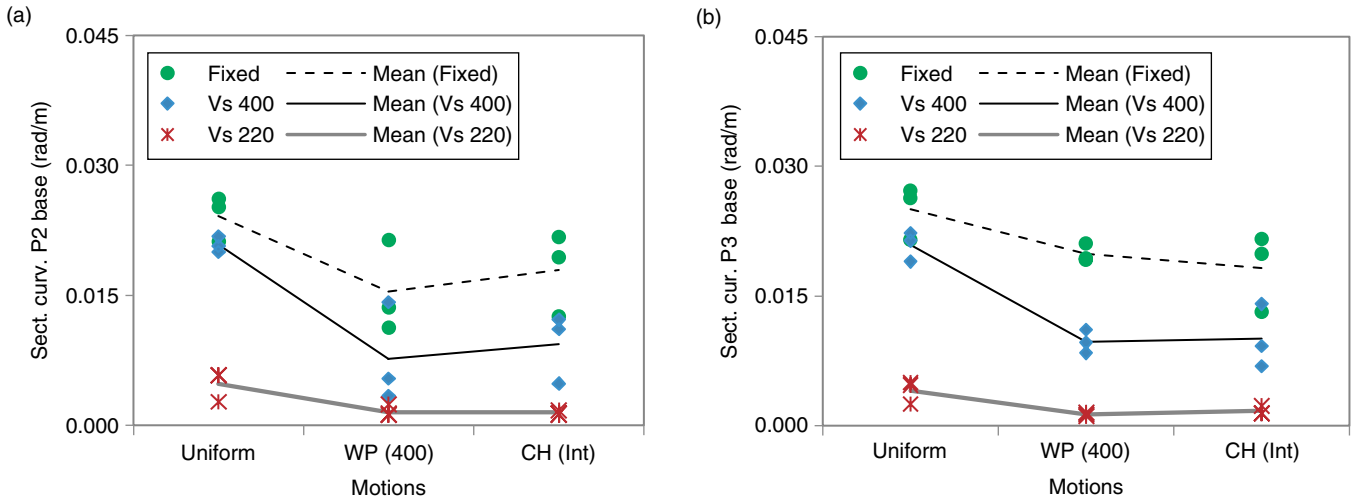


Figure 19. Comparison of section curvatures at base of: (a) Pier 2; and (b) Pier 3 of bridge model 1(a)

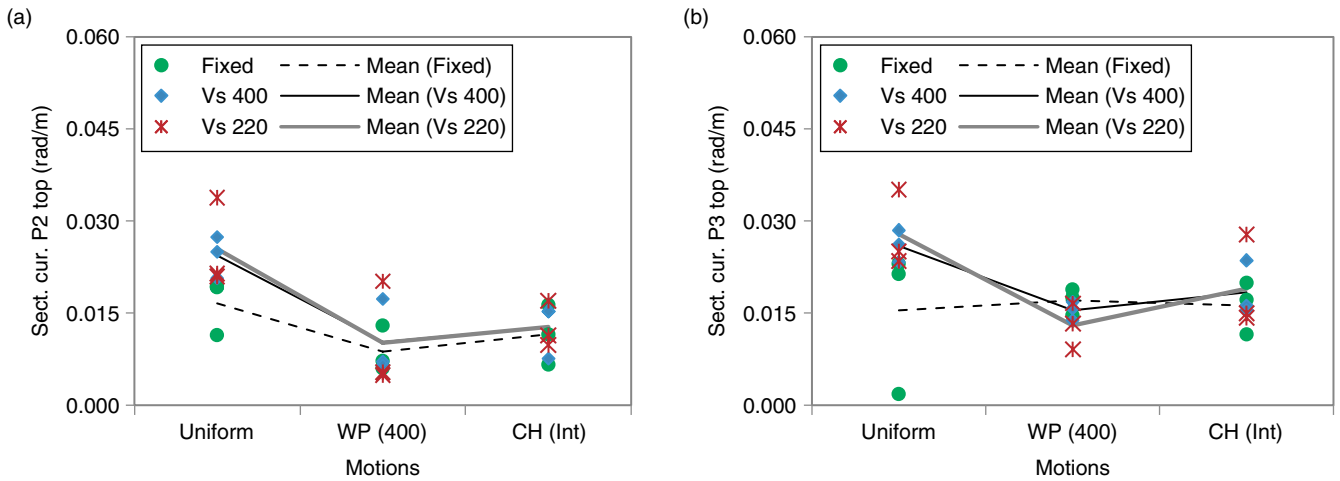


Figure 20. Comparison of section curvatures at top of: (a) Pier 2; and (b) Pier 3 of bridge model 1(a)

SSI could result in an increase of curvature demands at the top of the piers. The above observations demonstrate that the flexibility and additional damping introduced in the system by inclusion of soil spring benefits the response of piers by reducing the curvature demand at the base. On contrast, larger displacement demands resulting from SSI could result in an increase of curvature demand at the top of the bridge piers. Hence, in multiple frame bridges SSI could induce more damages at the top of the piers compared to the fixed base condition.

8. CONCLUSIONS

This paper presents parametric studies on the response of multiple-frame bridges with unseating restrainers to spatially varying ground motions and SSI. The nonlinear finite element model of multiple-frame

bridges includes pounding and energy dissipation during pounding, foundation flexibility and damping, frictions at supports, superstructure-abutment soil interaction and non-uniform ground motions to represent realistic bridge response. Based on the parametric studies conducted the following conclusions can be drawn:

- Spatially varying ground motion resulted in the reduction of the seismic demands on the piers of both stiff and flexible frames in the longitudinal direction. However, its effect on the relative responses such as relative hinge displacement, pounding forces and restrainer deformation are always detrimental. The present design method of the restrainers based on the uniform ground motion assumption could significantly underestimate the required stiffness and strength

of the restrainers to limit the joint opening movement. The numerical results indicate that the restrainers designed for uniform ground motion could suffer yielding or even fracturing under the influence of spatially varying ground motions.

- Adjusting the fundamental periods of the adjacent bridge components close to each other, as suggested by various codes, is indispensable to mitigate the relative displacement induced damages. However, this might not be sufficient to prevent the damages on bridge structures because of the relative displacements caused by inevitable ground motion spatial variations.
- Though SSI results in an increase in drift of the bridge frames, the relative displacement between the bridge frames at intermediate joints are reduced. This could be attributed to reduction of relative phasing of motion caused by the increase in flexibility of the frames due to the introduction of SSI. The SSI also benefits the response of bridge piers by reducing the curvature demands at the base of the piers. However, the larger displacement induced due to the SSI results in an increase in curvature demand at the top of the bridge piers.

It should be noted that in the present study the influences of multi-dimensional seismic excitations are not considered. As spatial ground motions also induce torsional responses, which may cause further relative displacement responses between adjacent bridge components, future studies with 3D bridge models are needed to consider the influence of all three components of ground motions on bridge response analysis.

ACKNOWLEDGEMENTS

The authors acknowledge the partial financial support from Australian Research Council Linkage project 110200906 for carrying out this research.

REFERENCES

- Bi, K. and Hao, H. (2012). "Modelling and simulation of spatially varying earthquake ground motions at sites with varying conditions", *Probabilistic Engineering Mechanics*, Vol. 29, pp. 92–104.
- Bi, K., Hao, H. and Chouw, N. (2011). "Influence of ground motion spatial variation, site condition and SSI on the required separation distances of bridge structures to avoid seismic pounding", *Earthquake Engineering & Structural Dynamics*, Vol. 40, No. 9, pp. 1027–1043.
- CALTRANS (2010). *Seismic Design Criteria: Design Manual-Version 1.6*, California Dept. of Transportation, Sacramento, CA, USA.
- Choi, E. (2002). *Seismic Analysis and Retrofit of Mid-America Bridges*, PhD Thesis, Georgia Institute of Technology, USA.
- Chouw, N. and Hao, H. (2003). "Effect of simultaneous spatial near-source ground excitation and soil on the pounding response of bridge girders", *Journal of Applied Mechanics*, Vol. 6, pp. 779–788.
- Chouw, N. and Hao, H. (2005). "Study of SSI and non-uniform ground motion effects on pounding between bridge girders", *Soil Dynamics and Earthquake Engineering*, Vol. 23, No. 7, pp. 717–728.
- Chouw, N. and Hao, H. (2008). "Significance of SSI and non-uniform near-fault ground motions in bridge response I: Effect on response with conventional expansion joint", *Engineering Structures*, Vol. 30, No. 1, pp. 141–153.
- Comartin, C.D., Greene, M. and Tubbesing, S.K. (1995). *The Hyogo-ken Nanbu Earthquake Jan 17, 1995*, EERI, Preliminary Reconnaissance Report, EERI-95-04, Oakland, CA, USA.
- Deodatis, G. (1996). "Non-stationary stochastic vector processes: seismic ground motion applications", *Probabilistic Engineering Mechanics*, Vol. 11, No. 3, pp. 149–167.
- Der Kiureghian, A. (1980). *A Response Spectrum Method for Random Vibrations*, Rep. No. UBC/EERC-80/15, Earthquake Engineering Research Centre, University of California Berkeley, USA.
- DesRoches, R. and Fenves, G.L. (2000). "Design of seismic cable hinge restrainers for bridges", *Journal of Structural Engineering*, ASCE, Vol. 126, No. 4, pp. 500–509.
- DesRoches, R. and Fenves, G.L. (2001). "Simplified restrainer design procedure for multiple-frame bridges", *Earthquake Spectra*, Vol. 17, No. 4, pp. 551–567.
- DesRoches, R. and Muthukumar, S. (2002). "Effect of pounding and restrainers on seismic response of multiple-frame bridges", *Journal of Structural Engineering*, ASCE, Vol. 128, No. 7, pp. 860–869.
- FEMA 356 (2000). *Pre-Standard and Commentary for the Seismic Rehabilitation*, American Society of Engineers, Virginia, USA.
- Feng, M.Q., Kim, J.M., Shinozuka, M. and Purusinghe, R. (2000). "Viscoelastic dampers at expansion joints for seismic protection of bridges", *Journal of Bridge Engineering*, ASCE, Vol. 5, No. 1, pp. 67–74.
- Gulkan, J. and Sozen, M. (1974). "Inelastic response of reinforced concrete structures to earthquake motion", *ACI Structural Journal*, Vol. 71, No. 2, pp. 604–610.
- Hao, H., Oliveira, C.S. and Penzien, J. (1989). "Multiple-station ground motion processing and simulation based on SMART-1 Array data", *Nuclear Engineering and Design*, Vol. 111, No. 3, pp. 293–310.
- Huo, Y. and Zhang, J. (2013). "Effects of pounding and skewness on seismic responses of typical multispan highway bridges using the fragility function method", *Journal of Bridge Engineering*, ASCE, Vol. 18, No. 6, pp. 499–515.
- Li, B., Bi, K., Chouw, N., Butterworth, J.W. and Hao, H. (2013). "Effect of abutment excitation on bridge pounding", *Engineering Structures*, Vol. 54, pp. 57–68.
- Japan Road Association (2004) *Specifications for Highway Bridges – Part V Seismic Design*, 5th ed, Japan Road Association, Japan. (in Japanese)

- Kawashima, K., Unjoh, S., Hoshikuma, J. and Kosa, K. (2011). ‘Damages of bridges due to the 2010 Maule, Chile, Earthquake’, *Journal of Earthquake Engineering*, Vol. 15, No. 7, pp. 1036–1068.
- Kim, J.M., Feng, M.Q. and Shinozuka, M. (2000). ‘Energy dissipating restrainers for highway bridges’, *Soil Dynamics and Earthquake Engineering*, Vol. 19, No. 1, pp. 65–69.
- Li, B., Bi, K., Chou, N., Butterworth, J.W. and Hao, H. (2012). ‘Experimental investigation of spatially varying effect of ground motions on bridge pounding’, *Earthquake Engineering & Structural Dynamics*, Vol. 41, No. 14, pp. 1959–1976.
- Mander, J.B., Nigel Priestley, M.J. and Park, R. (1988). ‘Theoretical stress-strain model for confined concrete’, *Journal of Structural Engineering*, ASCE, Vol. 114, No. 8, pp. 1804–1826.
- Martínez-Rueda, E.J. and Elnashai, A.S. (1997). ‘Confined concrete model under cyclic load’, *Materials and Structures*, Vol. 30, No. 3, pp. 139–147.
- Menegotto, M. and Pinto, P.E. (1973). ‘Method of analysis of cyclically loaded RC plane frames including changes in geometry and non-elastic behaviour of elements under combined normal force and bending’, *Symposium on the Resistance and Ultimate Deformability of Structures Acted on by Well Defined Repeated Loads*, IABSE, Zurich, Switzerland, pp. 15–22.
- Moehle, J.P. (1995). ‘Northridge Earthquake of January 17, 1994: reconnaissance report, Volume 1—highway bridges and traffic management’, *Earthquake Spectra*, Vol. 11, No. 4, pp. 287–372.
- Muthukumar, S. (2003). *A Contact Element Approach with Hysteresis Damping for the Analysis and Design of Pounding in Bridges*, PhD Thesis, Georgia Institute of Technology, USA.
- Muthukumar, S. and DesRoches, R. (2003). ‘A Hertz contact model with non-linear damping for pounding simulation’, *Earthquake Engineering Structural Dynamics*, Vol. 35, No. 7, pp. 811–828.
- Mylonakis, G., Sissy, N. and Gazetas, G. (2006). ‘Footing under seismic loading: Analysis and design issues with emphasis on bridge foundations’, *Soil Dynamics and Earthquake Engineering*, Vol. 26, No. 9, pp. 824–853.
- Richart, F.E. and Whitman, R.V. (1967). ‘Comparison of footing vibration tests with theory’, *Soil Mechanics Foundation Division*, ASCE, Vol. 93(SM6), pp. 143–168.
- Saiidi, M., Maragakis, E., Abdel-Ghaffar, S., Feng, S. and O’Connor, D. (1993). *Response of Bridge hinge Restrainers during Earthquakes-Field Performance, Analysis, and Design*, Report No. CCEER 93/06, Center for Civil Engineering Earthquake Research, University of Nevada, Reno, USA.
- Saiidi, M., Maragakis, E. and Feng, S. (1996) ‘Parameters in bridge restrainer design for seismic retrofit’, *Journal of Structural Engineering*, ASCE, Vol. 122, No. 1, pp. 61–68.
- Seismosoft Inc. (2012) *Seismo-Struct user Manual for Version 6*, USA.
- Sextos, A.G., Kappos, A.J. and Pitilakis, K.D. (2003). ‘Inelastic dynamic analysis of RC bridges accounting for spatial variability of ground motions, site effects and Soil-structure Interaction phenomena. Part 2: Parametric study’, *Earthquake Engineering & Structural Dynamics*, Vol. 32, pp. 629–652.
- Shrestha, B., Hao, H. and Bi, K. (2013). ‘Effectiveness of using Rubber bumper and restrainer on mitigating pounding and unseating damages of bridge structures subjected to spatially varying ground motions’, *Engineering Structures*, Vol. 79, pp. 195–210.
- Sobczyk, K. (1991). *Stochastic Wave Propagation*, Kluwer Academic Publishers, Netherlands.
- Trochalakis, P., Eberhard, M.O. and Stanton, J.F. (1997). ‘Design of seismic restrainers for in-span hinges’, *Journal of Structural Engineering*, ASCE, Vol. 123, No. 4, pp. 469–478.
- Won, J.H., Mha, H.S., Cho, K.I. and Kim, S.H. (2008) ‘Effects of the restrainer upon bridge motions under seismic excitations’, *Engineering Structures*, Vol. 30, No. 12, pp. 3532–3544.
- Zhang, J. and Markis, N. (2002a). ‘Kinematic response functions and dynamic stiffness of bridge embankment’, *Earthquake Engineering and Structural Dynamics*, Vol. 31, No. 11, pp. 1933–1966.
- Zhang, J. and Markis, N. (2002b). ‘Seismic response analysis of highway overcrossing including soil-structure interaction’, *Earthquake Engineering and Structural Dynamics*, Vol. 31, No. 11, pp. 1933–1966.

NOTATION

MRHD	Maximum relative hinge displacement
RD	Restrainer deformation
MRAD	Maximum relative abutment displacement
γ_{jk}	Coherency loss function between the ground motions at points j and k
d_{jk}	projected distance between points j and k in the wave propagation direction
α	incident angle of incoming wave to the soil site
β	coefficient depending on the level of coherency loss
v_{app}	apparent wave velocity
K_z	vertical stiffness of foundation
K_x	sway stiffness of foundation
K_{ry}	rocking stiffness of foundation
C_z	vertical viscous damping of foundation
C_x	sway viscous damping of foundation
C_{ry}	rocking viscous damping of foundation
G	shear modulus of soil
ρ	soil density
ν	Poisson’s ratio
V_s	shear wave velocity
V_{La}	Lysmer’s analog wave velocity
G_o	elastic shear modulus of soil
D_{eq}	relative hinge displacement
D_1	modal displacement of system 1
D_2	modal displacement of system 2
ρ_{12}	correlation coefficient between system 1 and system 2
β	ratio of the fundamental periods of two systems
ξ	modal damping of system

